

## A Structure–Reactivity Relationship for Single Walled Carbon Nanotubes Reacting with 4-Hydroxybenzene Diazonium Salt

Nitish Nair, Woo-Jae Kim, Monica L. Usrey, and Michael S. Strano\*

Contribution from the Department of Chemical and Biomolecular Engineering, University of Illinois at Urbana-Champaign, Urbana, Illinois 61801

Received November 9, 2006; E-mail: strano@uiuc.edu

**Abstract:** The first structure–reactivity relationship for electron-transfer reactions of single walled carbon nanotubes (SWNTs) has been derived and experimentally validated using 4-hydroxybenzene diazonium as a model electron acceptor. The model describes steady-state reaction data using an adsorption-controlled scheme, and electron transfer theories are used to explain the difference in reactivities between different nanotube chiralities. The formalism provides a mechanistic insight into electronically selective reactions. The influence of reagent concentration and external illumination ( $\sim 0.764$  mW/cm<sup>2</sup>) on the reaction selectivity is described by the rate model, with quantitative descriptions of the changes in the UV–vis–NIR absorption spectra of nanotubes during reaction. Illumination was shown to decrease the selectivity of the reagent to metallic SWNTs over semiconducting SWNTs. We attribute this to the greater activity of the reagent in solution when exposed to light, resulting in greater extents of reaction for each SWNT and, hence, lower selectivity.

### Introduction

Single-walled carbon nanotubes (SWNTs) are cylindrical graphene sheets,<sup>1,2</sup> with electronic structures determined by their chiralities.<sup>3</sup> Both metallic and semiconducting SWNTs have widespread applications in nanoelectronics and other areas.<sup>4,5</sup> These applications are limited by the fact that current synthetic methods produce SWNT mixtures of all electronic types.<sup>6</sup> We have previously reported selective chemical reactions using diazonium salts, which can covalently attach to metallic SWNTs, to the near exclusion of semiconducting SWNTs.<sup>7,8</sup> This selective reaction utilizes the difference in the population of electrons having energies near the Fermi level.<sup>7,8</sup> The selective chemistry can be used to manipulate the electronic properties of SWNT for nanotube field effect transistors<sup>9,10</sup> and as a chemical handle for electronic structure-based separation of SWNT mixtures. To achieve these goals, the reaction kinetics of each  $(n,m)$  SWNT as a function of its electronic band structure must be understood.

In order to estimate the relative reactivities of metallic and semiconducting nanotubes with 4-hydroxybenzene diazonium

salt, we used a semibatch reactor configuration in which the reagent was metered in at a precise rate. The SWNT absorption spectra were analyzed using a previously published deconvolution procedure,<sup>11</sup> which provided the surface coverage of diazonium on the SWNT as a function of the total amount of diazonium fed. We have shown in the past that the reaction of SWNTs with diazonium follows a two-step process:<sup>12</sup> a  $(n,m)$ -selective adsorption step followed by a covalent reaction step. The adsorption step is mediated by electron transfer from the nanotube<sup>13,14</sup> to the diazonium molecule, while the covalent bond results in the localization of electrons in its vicinity and the formation of an impurity state at the Fermi level.<sup>15,16</sup> Both processes lead to the reduction of peaks in the absorption spectrum. In constructing the rate equations for the coupled reactions, we have assumed that the adsorption step is rate-limiting. The nature of the semibatch setup is such that the diazonium concentration in the reactor is never allowed to accumulate. Due to these quasi-steady-state conditions, it is difficult to obtain dynamic information about the reaction; however, in a sample containing  $N$  nanotubes, we can reliably obtain the rate constants of  $N - 1$  nanotubes relative to the  $N^{\text{th}}$  nanotube, which yields a method of quantifying their relative reactivities.

- (1) Dresselhaus, M. S.; Dresselhaus, G.; Eklund, P. C. *Science of Fullerenes and Carbon Nanotubes*; Academic Press: San Diego, 1996.
- (2) Saito, R.; Dresselhaus, G.; Dresselhaus, M. S. *Physical Properties of Carbon Nanotubes*; Imperial College Press: London, 1998.
- (3) Bronikowski, M. J.; Willis, P. A.; Colbert, D. T.; Smith, K. A.; Smalley, R. E. *J. Vac. Sci. Technol., A* **2001**, *19*, 1800–1805.
- (4) McEuen, P. L. *Phys. World* **2000**, *13*, 31–36.
- (5) Tans, S. J.; Devoret, M. H.; Groeneveld, R. J. A.; Dekker, C. *Nature* **1998**, *394*, 761–764.
- (6) Ericson, L. M.; Pehrsson, P. E. *J. Phys. Chem. B* **2005**, *109*, 20276–20280.
- (7) Strano, M. S.; Dyke, C. A.; Usrey, M. L.; Barone, P. W.; Allen, M. J.; Shan, H. W.; Kittrell, C.; Hauge, R. H.; Tour, J. M.; Smalley, R. E. *Science* **2003**, *301*, 1519–1522.
- (8) Strano, M. S. *J. Am. Chem. Soc.* **2003**, *125*, 16148–16153.
- (9) An, L.; Fu, Q.; Lu, C.; Liu, J. *J. Am. Chem. Soc.* **2004**, *126*, 10520–10521.
- (10) Wang, C. J.; Cao, Q.; Ozel, T.; Gaur, A.; Rogers, J. A.; Shim, M. *J. Am. Chem. Soc.* **2005**, *127*, 11460–11468.

- (11) Nair, N.; Usrey, M. L.; Kim, W.; Braatz, R. D.; Strano, M. S. *Anal. Chem.* **2006**, *78*, 7689–7696.
- (12) Usrey, M. L.; Lippmann, E. S.; Strano, M. S. *J. Am. Chem. Soc.* **2005**, *127*, 16129–16135.
- (13) Zhao, J.; Lu, J. P. *Appl. Phys. Lett.* **2003**, *82*, 3746–3748.
- (14) Lu, J.; Nagase, S.; Zhang, X.; Wang, D.; Ni, M.; Maeda, Y.; Wakahara, T.; Nakahodo, T.; Tsuchiya, T.; Akasaka, T.; Gao, Z.; Yu, D.; Ye, H.; Mei, W. N.; Zhou, Y. *J. Am. Chem. Soc.* **2006**, *128*, 5114–5118.
- (15) Zhao, J.; Park, H.; Han, J.; Lu, J. *J. Phys. Chem. B* **2004**, *108*, 4227–4230.
- (16) Park, H.; Zhao, J.; Lu, J. P. *Nanotechnology* **2005**, *16*, 635–638.

The relative rate constants extracted from the data have been compared with those predicted by Marcus theory<sup>17,18</sup> and Gerischer–Marcus theory.<sup>19,20</sup> Marcus theory yields rate constants for electron transfer between donor and acceptor molecules as a function of (a) free energy of the electron-transfer step ( $\Delta G^\circ$ ) and (b) the reorganization energy ( $\lambda$ ) required to alter the atomic configurations of the reacting species so that isoenergetic electron transfer can take place in accordance with the Franck–Condon principle.<sup>17,21</sup> Gerischer–Marcus theory provides rate constants based on the convolution of the densities of states (DOS) of the acceptor and donor species.<sup>19,20</sup> Although this theory has been used for estimating rate constants of reactions at semiconductor electrodes<sup>19,20</sup> and at SWNT electrodes,<sup>22,23</sup> we have used it to examine trends in reactivities for SWNTs suspended in solution and, hence, extract relationships between SWNT electronic structures and their reactivities. While we have focused on electron-transfer reactions between SWNTs and 4-hydroxybenzene diazonium, the structure–reactivity expression derived in this work can be used for other molecules by suitably altering the redox potential term.

## Experimental Section

**Reactants.** HiPco SWNT (Rice University, HPR 107.1) were suspended in D<sub>2</sub>O with 1 wt % sodium dodecyl sulfate (SDS, Sigma-Aldrich). Ultrasonication was followed by ultra-centrifugation to individually suspend the SWNT following a previously published protocol.<sup>24</sup> The final concentration of SWNT in solution was approximately 9.3 wt %. The D<sub>2</sub>O was used to eliminate the contribution of water to the UV–vis–nIR absorption spectrum in the 1400–1770 nm wavelength range. 4-Hydroxybenzene diazonium tetrafluoroborate was chosen as the reagent instead of 4-chlorobenzene diazonium tetrafluoroborate, which was used in our previous study,<sup>7</sup> because the hydroxyl group aids in the electrophoretic separation of nanotube mixtures. The 4-hydroxybenzene diazonium salt was prepared by the reaction of nitrosonium tetrafluoroborate (NOBF<sub>4</sub>, Sigma-Aldrich) and 4-aminophenol (HO–C<sub>6</sub>H<sub>4</sub>–NH<sub>2</sub>, Sigma-Aldrich). Both reagents were dissolved in acetonitrile (Sigma-Aldrich) in a nitrogen environment. 4-Aminophenol solution was slowly added to the nitrosonium tetrafluoroborate solution at –20 °C (dry ice/acetone bath) for the reaction to proceed. The resultant diazonium salt was precipitated with the addition of diethyl ether, filtered, and dried under N<sub>2</sub> for 24 h. The diazonium salt was stored at –20 °C and dissolved into D<sub>2</sub>O immediately before the reaction.

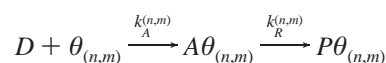
**Functionalization.** The SWNT–diazonium reaction was performed at pH 5.5 by injecting the diazonium salt solution with a syringe pump (Cole-Parmer) into a semibatch reactor containing the SWNT/SDS suspension. The total volume of the diazonium solution (500  $\mu$ L) was added at an injection rate of 20.83  $\mu$ L/h into a reactor volume of 5 mL under various diazonium concentrations. The reactor was well-stirred throughout the reaction time of 24 h. The functionalization of SWNTs

was controlled by varying the concentration of diazonium salt from 0 to 0.217 mol of diazonium/mol of carbon, at a reaction temperature of 45 °C. The influence of illumination by room light on the reaction rate and selectivity was also investigated at the diazonium concentration where the reaction selectivity for metallic SWNTs was maximized. The reacted SWNT solutions were characterized by UV–vis–nIR absorption spectroscopy (Shimadzu UV–310PC) to investigate the extent of reaction and selectivity.

## Model Development

We have developed a rate model for the reaction between the diazonium reagent and the nanotube sample. Only the relevant steps have been outlined below. A more detailed analysis is included in the supplement. After fitting the model to steady state absorption data, we obtained rate constants relative to the (11,5) nanotube, which had the maximum rate constant. In order to describe the trend in reactivities with band gap, we calculated rate constants relative to the (11,5) tube by using Marcus theory and Gerischer–Marcus theory. The use of both formalisms is predicated on the assumption that the adsorption step, which is mediated by charge transfer, is rate limiting.<sup>12</sup>

**Rate Equations.** Consider the following adsorption–reaction scheme,<sup>12</sup> for each (*n,m*) nanotube:



Here, *D* denotes the diazonium molecule, while  $\theta_{(n,m)}$ ,  $A\theta_{(n,m)}$ , and  $P\theta_{(n,m)}$  refer to the vacant sites on the nanotube, the sites occupied by the adsorption intermediate, and the sites occupied by the reaction product, respectively. The adsorption rate constant is  $k_A^{(n,m)}$ , and the reaction rate constant is  $k_R^{(n,m)}$ . An overall mass balance on the reactor gives its volume ( $V_R$ ) as a function of the initial volume ( $V_0$ ), volumetric flow rate of diazonium ( $\nu_0$ ), and time ( $t$ ), assuming that the density of the solution remains constant.

$$V_R = V_0 + \nu_0 t \quad (1)$$

A site balance carried out on the nanotube surface at any instant of time requires that the total number of sites ( $N_{T(n,m)}$ ) on a particular nanotube be the sum of the number of vacant sites ( $N_{\theta(n,m)}$ ) and those occupied by the adsorbed ( $N_{A\theta(n,m)}$ ) and reacted species ( $N_{P\theta(n,m)}$ ).

$$N_{T(n,m)} = N_{\theta(n,m)} + N_{A\theta(n,m)} + N_{P\theta(n,m)} \quad (2)$$

The final balance equations for diazonium and the adsorption/reaction sites on each SWNT can be simplified by assuming that the adsorbed intermediate ( $N_{A\theta(n,m)}$ ) is consumed as soon as it is generated and that the adsorption step is rate limiting ( $k_R^{(n,m)} \gg k_A^{(n,m)}$ ). The resulting expression for  $N_{A\theta(n,m)}$  is essential for the subsequent steps of the derivation.

$$N_{A\theta(n,m)} = \frac{k_A^{(n,m)}}{k_R^{(n,m)} V_R} N_D (N_{T(n,m)} - N_{P\theta(n,m)}) \quad (3)$$

When the reagent enters the reactor, it reacts with the SWNT to different extents, depending on whether they are metallic or semiconducting. The balance equations for the number of moles

- (17) Marcus, R. A. *J. Chem. Phys.* **1956**, *24*, 966–978.  
 (18) Bolton, J. R.; Archer, M. D. In *Electron Transfer in Inorganic, Organic and Biological Systems*; Bolton, J. R., Mataga, N., McLendon, G., Eds.; American Chemical Society: Washington, DC, 1991; pp 7–24.  
 (19) Gerischer, H. In *Physical Chemistry: An Advanced Treatise*; Eyring, H., Ed.; Academic Press, Inc: New York, 1970; Vol. 9A, pp 463–542.  
 (20) Bard, A.; Faulkner, L. R. *Electrochemical Methods, Fundamentals and Applications*, 2nd ed.; John Wiley and Sons: New York, 2001.  
 (21) Zwolinski, B. J.; Marcus, R. J.; Eyring, H. *Chem. Rev.* **1955**, *55*, 157–180.  
 (22) Heller, I.; Kong, J.; Heering, H. A.; Williams, K. A.; Lemay, S. G.; Dekker, C. *Nano Lett.* **2005**, *5*, 137–142.  
 (23) Heller, I.; Kong, J.; Williams, K. A.; Dekker, C.; Lemay, S. G. *J. Am. Chem. Soc.* **2006**, *128*, 7353–7359.  
 (24) O’Connell, M. J.; Bachilo, S. M.; Huffman, C. B.; Moore, V. C.; Strano, M. S.; Haroz, E. H.; Rialon, K. L.; Boul, P. J.; Noon, W. H.; Kittrell, C.; Ma, J. P.; Hauge, R. H.; Weisman, R. B.; Smalley, R. E. *Science* **2002**, *297*, 593–596.

of diazonium ( $N_D$ ) and the number of reacted sites on each nanotube ( $N_{P\theta_{(n,m)}}$ ) are respectively

$$\frac{dN_D}{dt} = F_{D_0} - \sum_{(n,m)} \frac{k_A^{(n,m)}}{V_R} N_D [N_{T_{(n,m)}} - N_{A\theta_{(n,m)}} - N_{P\theta_{(n,m)}}] \quad (4a)$$

$$\frac{dN_{P\theta_{(n,m)}}}{dt} = k_R^{(n,m)} N_{A\theta_{(n,m)}} \quad (4b)$$

In eq 4a,  $F_{D_0}$  denotes the molar flow rate of diazonium into the reactor. The magnitude of the rate of depletion of diazonium,  $r_D$ , is given by the sum on the right-hand side of the equation. The bracketed term is obtained from the site balance and represents the number of available sites on each nanotube. The above balances can be brought to their final forms with the aid of eq 3 and by defining the surface coverage on a  $(n,m)$  nanotube as  $\gamma_{(n,m)} = (N_{P\theta_{(n,m)}})/(N_{T_{(n,m)}})$ .

$$\frac{dN_D}{dt} = F_{D_0} - \frac{N_D}{V_R} \sum_{(n,m)} k_A^{(n,m)} N_{T_{(n,m)}} (1 - \gamma_{(n,m)}) \quad (5a)$$

$$\frac{d\gamma_{(n,m)}}{dt} = \frac{k_A^{(n,m)}}{V_R} N_D (1 - \gamma_{(n,m)}) \quad (5b)$$

Equation 5b is the general form for all nanotubes that participate in the reaction. In order to reduce the set of unknown parameters, the total number of sites on each nanotube ( $N_{T_{(n,m)}}$ ) is expressed as a fraction ( $\alpha_{(n,m)}$ ) of the total number of sites present in solution ( $N_T$ ).

$$N_{T_{(n,m)}} = \alpha_{(n,m)} N_T \quad (6a)$$

$$\alpha_{(n,m)} = \frac{A_{(n,m)}^\circ}{\sum_{(n,m)} A_{(n,m)}^\circ} \quad (6b)$$

The deconvolution of the absorption spectrum of an unreacted SWNT solution produces peak areas of the spectral profiles corresponding to each nanotube.<sup>11</sup> The peak area of a nanotube in the unreacted decant solution ( $A_{(n,m)}^\circ$ ) is postulated to be directly proportional to the total number of available reaction sites on that nanotube, since increasing the surface coverage decreases the peak area. Inherent in this statement are two further assumptions: (a) all nanotubes have the same extinction coefficient, and (b) surface coverage and absorbance are linearly related. When normalized to the total area, the ratio is assumed to give the fraction of sites for a particular nanotube.

**Time Scale.** The Damköhler Number ( $Da$ ) compares the characteristic times for reaction and convection.<sup>25</sup> When evaluated at the initial conditions,  $Da$  gives an estimate of the time scale for the reaction of diazonium.

$$Da = \frac{-r_D V_R}{F_{D_0}} \quad (7a)$$

where  $r_D$  is the rate of depletion of diazonium. Initially, all the sites on each nanotube are available for adsorption.

$$Da = \frac{\sum_{(n,m)} k_A^{(n,m)} \frac{N_D N_{T_{(n,m)}}}{V_R}}{C_{D_0} \nu_0} \quad (7b)$$

The numerator in eq 7b can be simplified via the following assumptions:

(a) Initially,  $N_D \approx C_{D_0} V_I$ , where  $C_{D_0}$  is the concentration of diazonium in the syringe, and  $V_I$  is the volume of diazonium solution injected into the reactor until that instant.

(b) The reactor volume changes negligibly initially, i.e.,  $V_0 \gg V_I$ , and, hence,  $V_R \approx V_0$ .

(c) Only the nanotube with the greatest adsorption rate constant ( $k_A^M$ ) contributes significantly to the summation.

Applying these assumptions leads to the following expression for  $Da$ .

$$Da = \frac{V_I k_A^M N_{T_M}}{V_0 \nu_0} = \frac{V_I / \nu_0}{V_0 / k_A^M N_{T_M}} = \frac{\tau_F}{\tau_R} \quad (7c)$$

In eq 7c,  $N_{T_M}$  is the total number of sites on the nanotube with the greatest rate constant,  $\tau_F$  is the amount of time spent by the reagent in the reactor, and  $\tau_R$  provides a time scale for the diazonium reaction. Since  $\tau_R$  was calculated by considering only the most reactive nanotube, it is an estimate of the instant at which the diazonium begins to react. Using eq 6b for the nanotube with the maximum rate, the final form of  $\tau_R$  can be expressed as

$$\tau_R = \frac{V_0}{k_A^M N_{T_M}} = \frac{V_0}{k_A^M \alpha_M N_T} \quad (7d)$$

**Nondimensional Analysis.** Equation 5a for the diazonium mole balance can be nondimensionalized by introducing a dimensionless time ( $t^* = t/\tau_R$ ) and a dimensionless molar amount of diazonium ( $\phi_D = N_D/N_T$ ). The reason for the latter normalization is that the total number of sites that the diazonium reagent can possibly occupy is  $N_T$ , and so,  $\phi_D$  varies between 0 and 1. The resulting nondimensional differential equation is

$$\frac{d\phi_D}{dt^*} = \frac{F_{D_0} \tau_R}{N_T} - \phi_D \frac{V_0}{V_R} \sum_{(n,m)} \frac{k_{(n,m)} \alpha_{(n,m)} (1 - \gamma_{(n,m)})}{k_M \alpha_M} \quad (8a)$$

where  $k_{(n,m)} = k_A^{(n,m)} N_T$  and  $k_M = k_A^M N_T$ . Equation 5b for the coverage on an  $(n,m)$  nanotube can be also nondimensionalized in the same manner.

$$\frac{d\gamma_{(n,m)}}{dt^*} = \phi_D \frac{k_{(n,m)} V_0 (1 - \gamma_{(n,m)})}{k_M V_R \alpha_M} \quad (8b)$$

The fit parameters are  $k_{(n,m)}$  and  $N_T$ . The nondimensional analysis naturally gives the reactivity of each nanotube relative to that of the most reactive nanotube, which is expected to be a metal. We report and correlate these ratios in this work.

(25) Fogler, H. S. *Elements of Chemical Reaction Engineering*, 3rd ed.; Prentice Hall, Inc.: New Jersey, 1999.

**Fermi Levels.** The position of the Fermi level ( $E_F$ ) relative to vacuum gives the work function ( $W$ ). If vacuum is taken to be zero, we have

$$E_F = -W \quad (9)$$

In the case of SWNTs, Okazaki et al. reported an inverse dependence of the work function on diameter.<sup>26</sup> Suzuki et al. ruled out significant diameter- and chirality-based differences in the work functions of metallic and semiconducting nanotubes.<sup>27</sup> More recent work has shown that nanotubes with diameters greater than 0.9 nm have work functions that asymptotically converge to the graphene limit (4.6 eV), while those with diameters less than 0.9 nm have diameter- and chirality-dependent work functions.<sup>28,29</sup> Since the diameter range of the nanotubes that we have considered for the reaction analysis extend from 0.757 to 1.375 nm, with most of the diameters exceeding 0.9 nm, we have assumed no chirality and diameter effects on the work function. From the tabulated work functions in ref 29, we have chosen  $W_{SWNT} = 4.45$  eV as a representative value for all nanotubes, thus giving  $E_F^{SWNT} = -4.45$  eV.

The half-wave potentials ( $E_{1/2}$ ) of various diazonium salts have been estimated using polarography.<sup>30</sup> We have assigned a value of 0.35 eV (SCE) to the redox potential of 4-hydroxybenzene diazonium salt. This assumes that it is at least as reactive with SWNTs as 4-chlorobenzene diazonium salt, for which  $E_{1/2}$  is available. The redox potential, referred to vacuum, is equivalent to the Fermi level of the redox species in solution.<sup>31,32</sup> The conversion from one scale to another can be performed as follows:<sup>20</sup>

$$E_F^D = -4.7 - V_{SCE} \quad (10)$$

which yields  $E_F^D = -5.05$  eV.

$E_F^{SWNT}$  can be fixed at the center of the gap<sup>28,29</sup> or, more generally, at the zero energy in the DOS of nanotubes. The redox level of diazonium relative to the zero energy of the nanotube DOS becomes  $-0.60$  eV.

**Marcus Theory.** The rate constant for an electron-transfer reaction ( $k_{ET}$ ) is a product of an attempt frequency ( $\nu_n$ ), a tunneling factor ( $\kappa_{el}$ ), and a nuclear factor ( $\kappa_n$ ).<sup>17,18,33</sup>

$$k_{ET} = \nu_n \kappa_{el} \kappa_n \quad (11a)$$

Tunneling can be neglected ( $\kappa_{el} \approx 1$ ) if the diazonium molecule is physically close to the nanotube during electron donation, i.e., the reaction is assumed to be adiabatic. The nuclear factor is quantified by Marcus theory in terms of the reorganization energy ( $\lambda$ ) and the free energy of the electron-transfer reaction ( $\Delta G^\circ$ ),<sup>17,18</sup> giving the following rate constant for an ( $n,m$ ) nanotube:

$$k_{ET}^{(n,m)} = \nu_n \exp\left(-\frac{(\lambda + \Delta G_{(n,m)}^\circ)^2}{4\lambda kT}\right) \quad (11b)$$

The electrochemical driving force,  $\Delta G_{(n,m)}^\circ$ , was linked to the band gap as follows:<sup>34,35</sup>

$$\Delta G_{(n,m)}^\circ = -\left(\left[E_F^{SWNT} - \frac{E_g^{(n,m)}}{2}\right] - E_F^D\right) \quad (11c)$$

where  $E_F^{SWNT}$  is the nanotube Fermi level and  $E_g^{(n,m)}$  is the band gap, which is zero for metallic tubes. The relative rate constant for an ( $n,m$ ) nanotube can be obtained by normalizing  $k_{ET}^{(n,m)}$  with respect to the maximum rate constant.

**Gerischer–Marcus Theory.** Gerischer–Marcus theory has been recently used to describe the kinetics of electrochemical reactions at SWNT electrodes.<sup>22,23</sup> We extend this formalism to electron-transfer reactions in solution by considering each suspended nanotube as an electrode. The rate constant for a certain nanotube depends on the convolution of its DOS ( $D_{(n,m)}(E)$ ) and the distribution of unoccupied redox states in solution ( $W_{ox}^{(n,m)}(E)$ ).<sup>19,20</sup>

$$k_{ET}^{(n,m)} = \nu_n \int_{E_F^D}^{E_F^{SWNT}} \epsilon_{ox}(E) D_{(n,m)}(E) W_{ox}^{(n,m)}(E) dE \quad (12a)$$

$$W_{ox}^{(n,m)}(E) = \frac{1}{\sqrt{4\pi\lambda kT}} \exp\left(-\frac{(\lambda + \Delta G_{(n,m)}^\circ)^2}{4\lambda kT}\right) \quad (12b)$$

The band structures of different carbon nanotubes were computed from tight-binding theory with the third nearest neighbor approximation.<sup>36,37</sup> The densities of states were calculated by the general expression provided by White and Mintmire for a 1-D system.<sup>38</sup> The tunneling term,  $\kappa_{el}$ , can be extracted from the proportionality function,  $\epsilon_{ox}(E)$ , and included in the integral prefactor.<sup>20</sup> Assuming that  $\epsilon_{ox}$  is independent of energy and that  $\nu_n$  and  $\epsilon_{ox}$  are not nanotube-specific, it follows that they cancel out when we calculate the relative rate constants.

**Selectivity.** The preference of diazonium toward metallic or semiconducting nanotubes can be measured by defining the reaction selectivity as the ratio of the total surface coverage for metallic SWNTs ( $\Gamma_{met}$ ) to that of the semiconductors ( $\Gamma_{sc}$ ). We have compared the selectivity predicted by the rate model ( $S_p$ ) to that obtained from the experimental data ( $S_e$ ).

$$S_p = \frac{\Gamma_{met}}{\Gamma_{sc}} \quad (13a)$$

Let  $M$  denote the set of all values of ( $n,m$ ) corresponding to metallic SWNTs, i.e., ( $n - m$ ) is divisible by 3. The following expressions can be derived for  $\Gamma_{met}$  and  $\Gamma_{sc}$  by using the definition of surface coverage,  $\gamma_{(n,m)} = (N_{p\theta_{(n,m)}})/(N_{T_{(n,m)}})$ , and eq 6a, which relates the total number of sites on each nanotube ( $N_{T_{(n,m)}}$ ) to the total number of sites in solution ( $N_T$ ).

(26) Okazaki, K.; Nakato, Y.; Murakoshi, K. *Phys. Rev. B* **2003**, *68*, 035434.

(27) Suzuki, S.; Watanabe, Y.; Homma, Y. *Appl. Phys. Lett.* **2004**, *85*, 127–129.

(28) Shan, B.; Cho, K. *Phys. Rev. Lett.* **2005**, *94*, 236602.

(29) Barone, V.; Peralta, J. E.; Uddin, J.; Scuseria, G. E. *J. Chem. Phys.* **2006**, *124*, 024709.

(30) Eloffson, R. M.; Gadallah, F. F. *J. Org. Chem.* **1968**, *34*, 854–857.

(31) Reiss, H. *J. Phys. Chem.* **1985**, *89*, 3783–3791.

(32) Gerischer, H.; Ekardt, W. *Appl. Phys. Lett.* **1983**, *43*, 393–395.

(33) Lewis, N. S. *Annu. Rev. Phys. Chem.* **1991**, *42*, 543–580.

(34) Strano, M. S.; Huffman, C. B.; Moore, V. C.; O’Connell, M. J.; Haroz, E. H.; Hubbard, J.; Miller, M.; Rialon, K. L.; Kittrell, C.; Ramesh, S.; Hauge, R. H.; Smalley, R. E. *J. Phys. Chem. B* **2003**, *107*, 6979–6985.

(35) O’Connell, M. J.; Eibergen, E. E.; Doorn, S. K. *Nat. Mater.* **2005**, *4*, 412–418.

(36) Reich, S.; Maultzsch, J.; Thomsen, C. *Phys. Rev. B* **2002**, *66*, 035412.

(37) Reich, S.; Thomsen, C.; Maultzsch, J. *Carbon Nanotubes*; Wiley-VCH: Weinheim, 2004.

(38) Mintmire, J. W.; White, C. T. *Phys. Rev. Lett.* **1998**, *81*, 2506–2509.

$$\Gamma_{met} = \frac{\sum_{(n,m) \in M} N_{P\theta_{(n,m)}}}{\sum_{(n,m) \in M} N_{T_{(n,m)}}} = \frac{\sum_{(n,m) \in M} \gamma_{(n,m)} \alpha_{(n,m)}}{\sum_{(n,m) \in M} \alpha_{(n,m)}} \quad (13b)$$

$$\Gamma_{sc} = \frac{\sum_{(n,m) \notin M} N_{P\theta_{(n,m)}}}{\sum_{(n,m) \notin M} N_{T_{(n,m)}}} = \frac{\sum_{(n,m) \notin M} \gamma_{(n,m)} \alpha_{(n,m)}}{\sum_{(n,m) \notin M} \alpha_{(n,m)}} \quad (13c)$$

The experimental reaction selectivity ( $S_e$ ) is obtained by taking the ratio of the overall degrees of functionalization for metallic ( $\delta_{met}$ ) and semiconducting SWNTs ( $\delta_{sc}$ ).

$$S_e = \frac{\delta_{met}}{\delta_{sc}} \quad (14a)$$

All metallic SWNTs are grouped into one unit, and all the semiconductors into a second. For each group, the degree of functionalization is defined as

$$\delta_{met,sc} = \frac{A_{initial}^{met,sc} - A_{unreacted}^{met,sc}}{A_{initial}^{met,sc}} \quad (14b)$$

where  $A_{initial}^{met,sc}$  is the area under the metallic or semiconducting region of the absorption spectrum of the starting SWNT solution, and  $A_{unreacted}^{met,sc}$  is the area under the corresponding region after reaction.

## Results

Reactions of SWNTs with 4-hydroxybenzene diazonium salt were performed at various diazonium concentrations and temperatures, with and without illumination of visible light. The UV–vis–nIR absorption spectra were collected for each sample after reaction. The spectral contributions of carbonaceous species and unreacted diazonium salt were eliminated by background subtraction.

**Functionalization.** Figure 1a and b show UV–vis–nIR absorption spectra of deuterated SWNT solutions reacted with increasing concentrations of 4-hydroxybenzene diazonium at 45 °C, with and without illumination. The reagent concentrations have been expressed as moles of diazonium per moles of carbon (D/C). The absorption features represent Van Hove transitions of each  $(n,m)$  SWNT at different wavelengths. The first Van Hove transitions of metallic species ( $E_{11}^M$ ) appear between 440 and 645 nm, while the first ( $E_{11}^S$ ) and second ( $E_{22}^S$ ) Van Hove transitions of semiconducting species appear within 830–1600 nm and 600–800 nm, respectively. When the SWNTs are covalently functionalized by diazonium salts, their absorption peaks diminish because electrons are localized by the formation of a covalent bond.<sup>12,15,16</sup> This enables the monitoring of the extent of adsorption/reaction for each  $(n,m)$  nanotube.

Figure 1a shows that there are no significant changes in the absorption features of all individual SWNTs until 0.019 D/C diazonium solution is added. When the concentration of added diazonium solution exceeds 0.027 D/C, notable changes in the absorption features are observed. The  $E_{11}^M$  peak intensities start to decrease, while those representing the  $E_{11}^S$  and  $E_{22}^S$  transi-

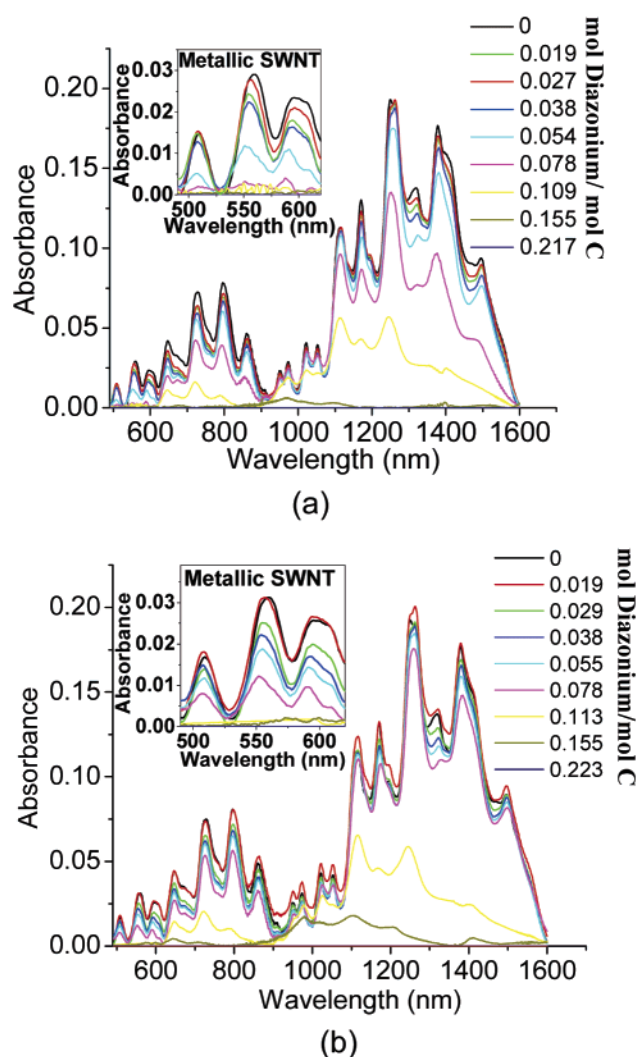


**Figure 1.** Photoabsorption spectra of SWNTs reacted with 4-hydroxybenzene diazonium (a) under illumination and (b) in the dark. Diazonium concentrations, normalized to the number of carbons, are listed in the figures. For each of the listed concentrations, 500  $\mu$ L of 4-hydroxybenzene diazonium salt dissolved in  $D_2O$  were injected into 5 mL of SWNT solution over the course of 24 h, at 45 °C and a pH of 5.5. The insets in (a) and (b) show the decay of the metallic peaks with increasing diazonium content.

tions of the semiconducting species show little change. This indicates that metallic SWNTs react with the diazonium salt before the semiconducting SWNTs. This trend becomes more prominent at the diazonium concentration of 0.054 D/C, where half the metallic SWNTs have reacted, while most of the semiconducting SWNTs still remain unreacted. At 0.078 D/C, most of the metallic SWNTs have been functionalized, and semiconducting SWNTs with large diameters (0.93–1.25 nm) begin to react. At high concentrations of diazonium solution (>0.155 D/C) all nanotubes react, regardless of electronic structure, resulting in the complete decay of all absorption features.

The reactivities of SWNTs in the absence of illumination show a different trend, as shown in the SWNT absorption spectra in Figure 1b. At a concentration of 0.078 D/C, significant amounts of metallic SWNT still remain unreacted, in contrast to the illuminated reaction. The effect of illumination on the extents of reaction of SWNTs may originate from the different

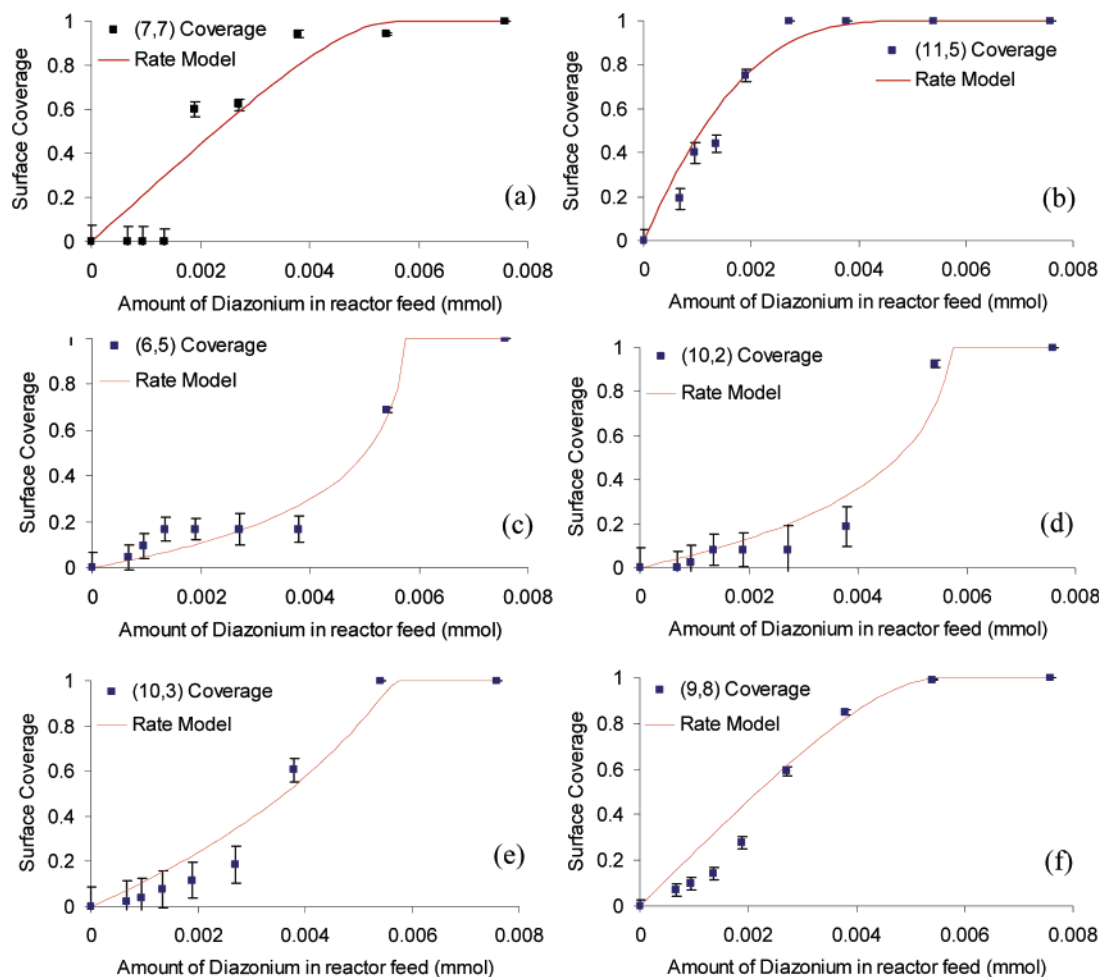


**Figure 2.** Surface coverage ( $\gamma_{(n,m)}$ ) as a function of the total amount of diazonium fed into the 5 mL reactor for representative metallic and semiconducting nanotubes in the light reaction. The black squares denote the surface coverage data obtained from the deconvolution of the absorption spectra of the SWNT–diazonium reactions, and the red lines represent the fits predicted by the adsorption-based rate model.

reactivities of the diazonium intermediate radical, whose form changes upon illumination.<sup>39</sup> The diazonium is known to form two types of radicals: the diazenyl radical ( $\text{Ar}-\text{N}=\text{N}\bullet$ ) and the aryl radical ( $\text{Ar}\bullet$ ), where Ar denotes an aromatic group. The latter is known to be the major intermediate when the diazonium is exposed to illumination. Based on the reaction results in Figure 1a and b, the presence of excess aryl radicals, in addition to diazenyl radicals, leads to greater extents of reaction in the illuminated case.

The above results confirm that electronic structure selective chemistry on nanotubes can be performed with 4-hydroxybenzene diazonium. The preference of diazonium toward metallic or semiconducting SWNTs can be gauged through the selectivity parameter, which we have defined as the ratio of the total extent of reaction of metallic SWNTs to that of the semiconductors. The effects of diazonium concentration and illumination on the selectivity are explored in the following section.

## Discussion

**Approximation.** Spectral line shapes corresponding to at least 56 nanotubes (18 metals + 38 semiconductors) constitute the absorption spectrum of SDS-suspended HiPco SWNTs. Strictly speaking, in eq 8a and b, 56 values of  $k_{(n,m)}$  should be used as

fit parameters; however, as described in ref 11, each absorption peak is composed of nanotubes with similar transition energies. We used a simple weighting scheme to approximate the spectral contribution of each  $(n,m)$  species to the parent peak. The upshot in reaction analysis is that the absorption peaks of all nanotubes comprising the parent peak decrease at the same rate with increasing diazonium content. In other words, nanotubes with comparable transition energies are observed to have similar reactivities. Across the wavelength range considered (490–1600 nm), we have examined the effect of diazonium on 17 representative nanotubes (4 metals + 13 semiconductors) whose transition energies lay closest to the corresponding absorption peaks. The depletion of these peaks is due to the presence of adsorbed and covalently bonded diazonium molecules on each nanotube.<sup>12</sup> Therefore, the surface coverage introduced in eqs 5a and b ( $\gamma_{(n,m)}$ ) can also be interpreted as

$$\gamma_{(n,m)} = \frac{A_{(n,m)}^{\circ} - A_{(n,m)}^N}{A_{(n,m)}^{\circ}} \quad (15)$$

where  $A_{(n,m)}^{\circ}$  is the peak area of an  $(n,m)$  nanotube in the unreacted decant, and  $A_{(n,m)}^N$  is the depleted peak area of the same nanotube at the completion of the  $N^{\text{th}}$  addition of diazonium.

(39) Griffiths, J.; Murphy, J. A. *J. Chem. Soc., Chem. Commun.* **1992**, 24–26.

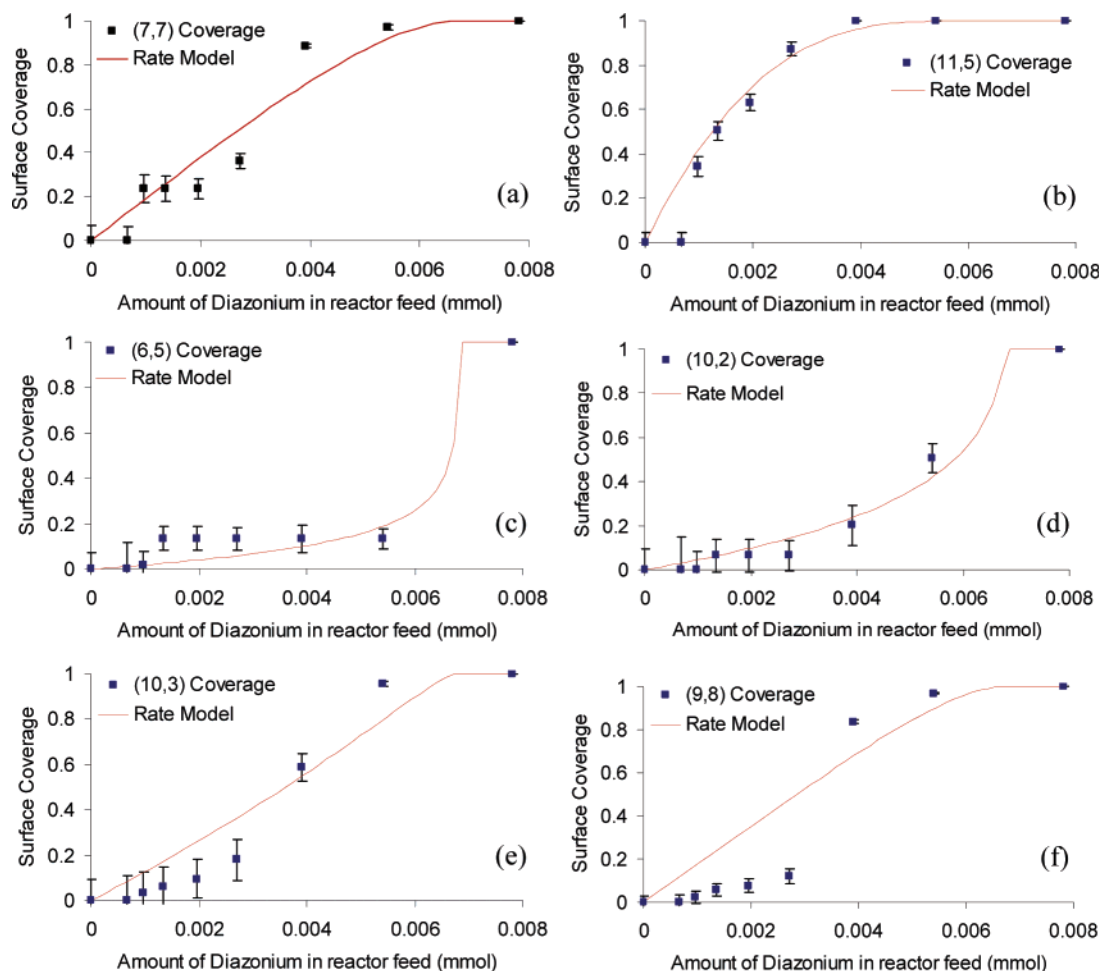


**Figure 3.** Surface coverage ( $\gamma_{(n,m)}$ ) as a function of the total amount of diazonium fed into the 5 mL reactor for representative metallic and semiconducting nanotubes in the dark reaction. The black squares denote the surface coverage data obtained from the deconvolution of the absorption spectra of the SWNT–diazonium reactions, and the red lines represent the fits predicted by the adsorption-based rate model.

**Table 1.** Relative Rate Constants for Metallic Nanotubes as Obtained from the Spectral Fits, Marcus Theory, and Gerischer–Marcus Theory<sup>a</sup>

$(n,m)$	relative rate constants (dark)			relative rate constants (light)		
	spectral fits	Marcus theory	Gerischer–Marcus theory	spectral fits	Marcus theory	Gerischer–Marcus theory
(7,7)	$0.388 \pm 0.108$	1.000	0.143	$0.389 \pm 0.086$	1.000	0.143
(10,4)	$0.577 \pm 0.164$	1.000	0.500	$0.652 \pm 0.146$	1.000	0.500
(11,5) <sup>b</sup>	1.000	1.000	1.000	1.000	1.000	1.000
(11,8)	$0.344 \pm 0.094$	1.000	1.000	$0.408 \pm 0.087$	1.000	1.001

<sup>a</sup> Figure 4a and b show that the electron transfer theories can explain the trend in the relative rate constants with band gap for semiconductors. While the theories predict higher relative rate constants for metallic SWNTs than for semiconducting SWNTs, they fail in detecting trends among the metals themselves.  
<sup>b</sup> All rate constants were calculated relative to the (11,5) nanotube.

**Fit Results.** The predictions of the rate model are able to reproduce the surface coverage data obtained from the deconvoluted absorption spectra. The  $(n,m)$ -specific fits in Figures 2 and 3 show the results for two metals ((7,7) and (11,5)), two small-diameter semiconductors ((6,5) and (10,2)), and two large-diameter semiconductors ((9,8) and (10,3)). The total number of sites in solution ( $N_T$ ) was computed as 0.00574 and 0.00684 mmol for the light and dark reactions, respectively. The approximate concentration of SWNTs in the starting solution was 9.3 wt %. In the 5 mL reactor volume, this translates to 0.0347 mmol of carbon atoms. The total number of sites computed is at least an order of magnitude lower than the number of carbons present in solution, which means that not

all the carbon atoms are reactive sites. It can be seen that the metals react at low amounts of diazonium, while the semiconductors typically react after a delay. Once it was known that the (11,5) nanotube had the highest rate constant ( $k_{(11,5)}$ ), the fitting procedure was repeated by keeping  $k_{(11,5)}$  invariant and determining the rate constants of the other nanotubes relative to it. The 95% confidence intervals for these parameter estimates were calculated with the underlying assumption that  $k_{(11,5)}$  was accurately known. The gradient in rate constants between the various reacting species causes the metal  $\rightarrow$  large-diameter semiconductor  $\rightarrow$  small-diameter semiconductor progression. The precise metering of the diazonium reagent into the reactor ensures that this progression is maintained. An excess would

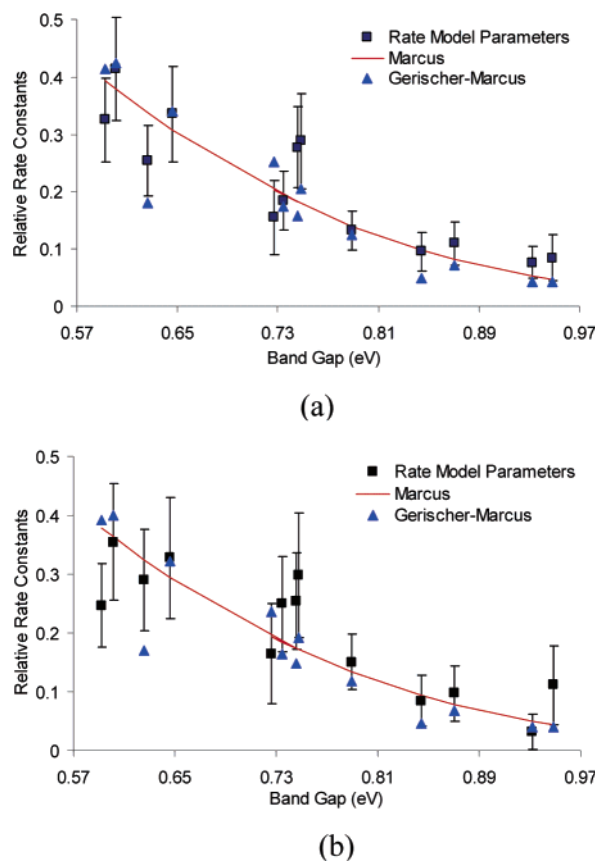


**Figure 4.** Comparison of the computed relative rate constants (fit parameters obtained from the surface coverage data, along with their associated 95% confidence intervals) for the semiconductors with the predictions of the Marcus and Gerischer–Marcus theories for the (a) light and (b) dark reactions. Both electron transfer theories predict the expected dependence of relative rate constants on band gap, i.e., large band gap (small-diameter) semiconductors react slower than small band gap (large-diameter) semiconductors.

lead to a semiconductor reaction as well, thus obscuring any difference in rate constants among the reacting nanotubes.

**Structure–Reactivity.** The electronic structure–reactivity relationship for nanotubes can be explained by using the Marcus and Gerischer–Marcus formalisms to fit the relative rate constant data. The comparison between the fitted ( $k_{(n,m)}$ ) and theoretically estimated ( $k_{ET}^{(n,m)}$ ) relative rate constants for semiconducting SWNTs is shown in Figure 4a and b, along with the associated 95% confidence intervals for the former. The sole fit parameter, the reorganization energy ( $\lambda$ ), was estimated as 0.54 eV by Marcus theory and 0.71 eV by Gerischer–Marcus theory. These values lie between the observed bounds for  $\lambda$  (0.5 and 1 eV).<sup>20</sup> Despite the scatter, the expected trend is obtained for the semiconductors: large-diameter semiconductors have higher relative rate constants than their small-diameter counterparts. Metallic nanotubes have higher rate constants than the semiconductors due to the finite DOS at the Fermi level, which is conducive to electron transfer. Although this is predicted by the Marcus and Gerischer–Marcus theories, the model and data values do not agree as well for the metallic nanotubes (Table 1). This difference could be attributed to the reaction step, which we have assumed as non-rate-limiting.

The relative rate constants have been correlated with the band gaps instead of the SWNT diameters. This is because the band

gaps play a more significant role in determining the values of the relative rate constants. The electrochemical driving force defined in eq 11c depends on the position of the first Van Hove singularity in semiconducting nanotubes, relative to the redox potential of diazonium. The larger the band gap, the smaller the driving force and, hence, the smaller the rate constant. The rate constant according to Gerischer–Marcus theory (eq 12a) depends on the convolution of the densities of states of the reacting species. The larger the band gap, the larger the region where the SWNT DOS is zero, which leads to a smaller overlap between the densities of states of the nanotube and the diazonium molecule. In an SWNT–diazonium reaction mixture where different ( $n,m$ ) nanotubes are present, the charge-transfer-mediated adsorption step could be rate limiting because a spectrum of energy states is available for electron donation; this, along with the metal  $\rightarrow$  large-diameter semiconductor  $\rightarrow$  small-diameter semiconductor progression observed experimentally, also rationalizes the dependence of the relative rate constants on the band gap.

**Reaction Selectivity.** The reaction selectivity has been defined as the ratio of the overall degrees of functionalization of metallic ( $\delta_{met}$ ) and semiconducting SWNTs ( $\delta_{sc}$ ). The effect of illumination on  $\delta_{met}$  and  $\delta_{sc}$ , as shown in Figure 5a, is to increase the extents of reaction and the rates for metals and semiconductors at all concentrations of the reagent. We expect the enhanced conversion to lower the selectivity in the light when compared to the dark. This is evident in Figure 5b and c, which depict the experimentally observed ( $S_e$ ) and theoretical selectivities ( $S_p$ ), respectively, for each input of diazonium. Although a similar trend is seen in both figures, there are discrepancies in the magnitudes of  $S_e$  and  $S_p$ . This can be attributed to the relatively low quality of the fit for large-diameter semiconductors at low diazonium concentrations in the dark (Figure 3e and f). Due to an overestimation of the surface coverage of large-diameter semiconducting SWNTs in the dark reaction, the rate model underestimates its selectivity. Consequently, the difference in light and dark selectivities in the low reagent concentration regime (Figure 5c) is much lower than that in reality (Figure 5b).

We stated previously that illumination raised the overall reaction rate, thus resulting in greater conversion. An increase in the rate can be due to either higher rate constants for the nanotubes or a higher activity of diazonium in solution. A parity plot between the light and dark relative rate constants in Figure 5d shows that they are similar, with limited dispersion (standard deviation = 0.0417) about a line with unit slope. With the inclusion of confidence intervals,<sup>40</sup> we see that the relative rate constants for the two cases are not statistically different from each other, thus leading to two possibilities: (a) the absolute rate constants do not change at all in the presence of light, and (b) a uniform increase in the rate constants of all the nanotubes occurs in such a way as to maintain the same relative ratios. Illumination causes the diazonium to decompose into aryl radicals, the concentrations of which are negligible in the dark. The presence of an excess of reactive radicals,  $\text{Ar-N=N}\cdot$  and  $\text{Ar}\cdot$ , increases the activity of diazonium in solution and, hence, the reaction rate. All these factors contribute to greater degrees of functionalization for each ( $n,m$ ) SWNT in the presence of illumination, thereby decreasing the selectivity.

(40) See Supporting Information.



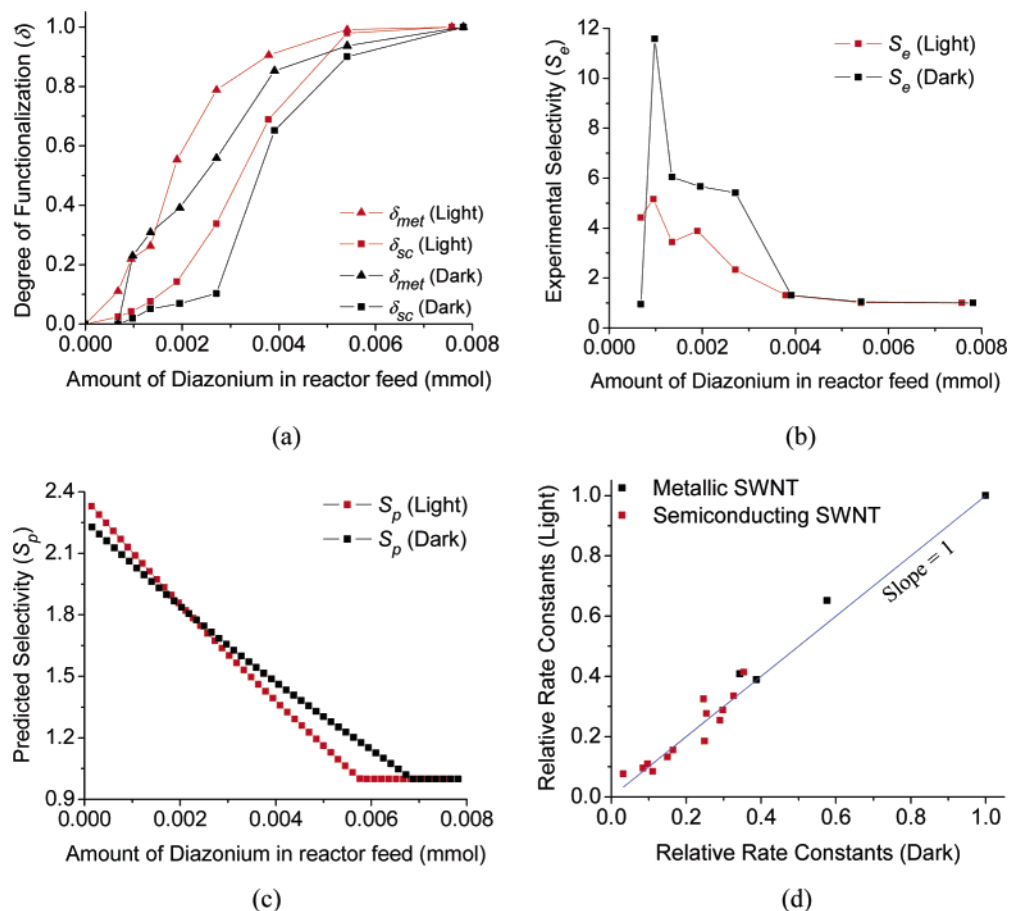


**Figure 5.** (a) A composite plot comparing the degrees of functionalization of metallic ( $\delta_{met}$ ) and semiconducting ( $\delta_{sc}$ ) SWNTs in the light and dark. (b and c) Experimental and theoretical selectivities, respectively, as functions of the total amount of diazonium fed. The light reaction has a lower selectivity due to higher extents of reaction for all nanotubes. The rate model overestimates  $\delta_{sc}$  for large-diameter semiconductors at low concentrations of diazonium in the dark reaction, thus leading to a mismatch with the observed trend. (d) A comparison of relative rate constants for the light and dark shows that they are similar, indicating that illumination does not preferentially enhance the rate constant for a particular ( $n,m$ ) species over another.

## Conclusion

We have presented a structure–reactivity relationship for reactions of HiPco SWNTs with 4-hydroxybenzene diazonium salt. Subsequent deconvolution of the reaction spectra yielded surface coverage of the diazonium on the nanotubes as a function of the total molar amount of diazonium added. A rate model for the steady-state data that considered the adsorption step as rate-limiting was used to extract rate constants normalized to the (11,5) nanotube. Illumination results in the photodecomposition of diazonium into reactive aryl radicals. The increased activity of the reagent in the light leads to greater extents of reaction for all nanotubes and, therefore, a lower overall selectivity when compared to the dark reaction. The relative rate constants were found to vary little due to illumination.

**Acknowledgment.** The authors would like to thank A. Bezryadin and C. Fantini for insights on the calculation of the density of states of carbon nanotubes from their band structures, and R. D. Braatz for useful discussions concerning the rate equations. We are also grateful to P. W. Barone and C. Y. Lee for suggestions and amendments to the manuscript. This work was supported by the Korea Research Foundation Grant funded by the Korean Government (MOEHRD) (KRF-2005-214-D00260), the Intel Grant, and NSF-Career.

**Supporting Information Available:** The detailed derivation of the rate model and plots of the relative rate constants for the light and dark (with the 95% confidence intervals). This material is available free of charge via the Internet at <http://pubs.acs.org>.

JA068018I